

Effect of the incorporation of lignin microparticles on the properties of the thermoplastic starch/pectin blend obtained by extrusion

Danielly de Oliveira Begali ^{a,*}, Laura Fonseca Ferreira ^a, Ana Carolina Salgado de Oliveira ^a, Soraia Vilela Borges ^a, Alfredo Rodrigues de Sena Neto ^b, Cassiano Rodrigues de Oliveira ^c, Maria Irene Yoshida ^d, Claire I.G.L. Sarantopoulos ^e

^a Food Science Department, Federal University of Lavras, P.O. Box 3037, 37200-900 Lavras, MG, Brazil

^b Engineering Department, Federal University of Lavras, P.O. Box 3037, 37200-900 Lavras, MG, Brazil

^c Institute of Exact and Technological Sciences, Federal University of Viçosa, Rio Paranaíba, MG 38810-000, Brazil

^d Department of Chemistry, Federal University of Minas Gerais, 31270-901 Belo Horizonte, MG, Brazil

^e Institute of Food Technology, Packaging Technology Center, 13070-178 Campinas, SP, Brazil

ARTICLE INFO

Article history:

Received 29 December 2020

Received in revised form 1 March 2021

Accepted 13 March 2021

Available online 15 March 2021

Keywords:

Extrusion

Biodegradable

Antioxidant

ABSTRACT

The present study aimed to produce thermoplastic starch films with different concentrations of thermoplastic pectin and the addition of 4% lignin microparticles as a reinforcing and active agent. The pectin improved the modulus of elasticity, and decreased the elongation at break. In addition, it improved the UV light protection to 100% at 320 nm and 95.9% at 400 nm. The incorporation of lignin microparticles improved the thermal stability of the blends made with 25% and 50% thermoplastic pectin when compared to the pectin-free blends. The blend with 25% thermoplastic pectin led to an increase of 75.8% and 34% in elongation at break and deformation of the films, respectively. This blend also improved the UV light protection to 100% due to its dark brown color. Regarding the permeability properties, the films with 25% and 50% thermoplastic pectin showed lower oxygen permeability (48% and 65%) and an increase in the antioxidant activities from 2.7% to 71.08% and 4.1% to 79.28%, respectively. Thus, the polymer blend with 25% thermoplastic pectin with the incorporation of lignin microparticles proved to be a good alternative for use in foods sensitive to the effects of oxygen and UV light.

© 2021 Elsevier B.V. All rights reserved.

1. Introduction

Starch and pectin are natural polymers that have aroused the interest of researchers and food industries for the production of biodegradable films, as they are renewable, non-toxic, low-cost, and widely available resources. In the case of pectin, it can be extracted from citrus fruit residues. In addition, these two polymers can be produced by the extrusion technique, which allows a large-scale simulation of the use of biopolymer films [1,2].

Starch films are transparent, odourless, colorless and have low oxygen permeability. However, they are weak mechanical properties and are brittle [2,3]. The films obtained from pectin, on the other hand, have good gas barrier properties and delay lipid migration, however, they have high permeability to water vapor [4,5]. In this way, it appears that it is necessary to study the mixture of polymers for the production of films with better properties.

Furthermore, an effective alternative to improve the properties of biodegradable films is the use of reinforcing agents, such as lignin, which consists of a complex macromolecule found in plants along with cellulose and hemicellulose. This molecule has been used in the production of films to improve the mechanical and thermal properties and partially block the UV light and the antioxidant activity. These properties are due to the presence of different functional groups in the lignin molecule structure, which varies according to the botanical origin [6–9]. Lignin also has intrinsic properties, such as a high degree of cross-linking, hydrophobicity, and an amorphous and three-dimensional structure that make it attractive for several applications [8,10].

So far, no studies have focused on films made with starch, pectin, and lignin produced by the extrusion technique. In turn, starch-based films made by casting technique have already been studied, such as starch/pectin [1,11–14] and starch/lignin-based films [10,15]. However, there are few studies on films obtained by extrusion, including starch/pectin [16,17] and starch/lignin-based films [18], while pectin/lignin blends have been investigated only for the production of hydrogels as biomedical materials [19]. Thus, the objective of this study was to evaluate the properties of thermoplastic starch/pectin films, with the

* Corresponding author.

E-mail address: danibegali@gmail.com (D. de Oliveira Begali).

incorporation of lignin microparticles, since the mixture of these materials was not found in the research already carried out.

2. Material and methods

2.1. Material

The following ingredients were used to produce the films: starch (406 R03; Cassava S/A); high methoxylation pectin (75.7%; Dinâmica Química); glycerol (99.5%; Sigma-Aldrich); stearic acid (95%; Êxodo Científica); citric acid (99.7%; Proquimios Comércio and Indústria Ltda). Lignin isolated from black kraft liquor was kindly donated by the Laboratory of Bioactive Product Development and Technological Solutions at the Federal University of Viçosa (Rio Paranaíba Campus). The reagents methanol (Vetec), and 2,2-diphenyl-1-picryl-hydrazyl (DPPH; Sigma Aldrich) were also used.

2.2. Methods

2.2.1. Synthesis of lignin microparticles (MPL)

For the production of the lignin microparticles (MPL), a TE-350 ball mill with a video camera was used (Tecnal, São Paulo, Brazil). For that, 10 g of sample was placed in the enclosed container together with steel balls attached to the equipment and agitated for 2 min. The procedure was repeated 3 times to obtain the lignin microparticles. The particle size reduced from 6.6 μm to 3.1 μm . The MPL concentration used in the film formulations was established by pre-tests.

2.2.2. Production of the films

For all formulations, an SJSJL 20 NZ model twin-screw extruder was used (40/1 L/D, and 20 mm of screw diameter, D) at 100 rpm, varying only the temperature profile.

Thermoplastic starch was obtained according to the methodology described by Ferreira et al. [20]. The starch was dried in an oven at 45 °C for 24 h (60% w/w in relation to the total mass). Then, it was mixed with glycerol (24% w/w in relation to the total mass) used as a plasticizer, distilled water (14% w/w), stearic acid (1% w/w) as a flow agent, for facilitating the fluidity of the starch inside the extruder and citric acid (1% w/w) to protect the material to be extruded from oxidation. The mixture was cooked by extrusion under various temperature combinations (80, 80, 90, 90, 100, 100 and 110 °C) and then extruded at 120 rpm, with a 2 mm size matrix. The extruder generates filaments that were pelletized to a length of 3 mm and a diameter of 3.2 mm. The pelleted material was stored until blends were prepared [21].

To obtain the thermoplastic pectin (TPP) used the methodology described by De Oliveira et al. [22], pectin (49% w/w relative to the total mass) was mixed with glycerol (25% w/w relative to the mass of pectin) used as a plasticizer, distilled water (30% v/v), and citric acid (1.5% w/w) to lower the pH, relative to the total mass. Then, it was extrusion cooked at various temperatures (35, 50, 75, 90, 100, 100, and 90 °C), extruded, and stored until the preparation of the blends [21].

Subsequently, the TPS and TPP pellets were mixed with and without the incorporation of 4% of lignin microparticles (relative to the mass of starch and pectin) were extruded at different temperatures (50, 70, 75, 85, 90, 100, and 100 °C). The TPS, TPP, and MPL concentrations used in the formulations are shown in Table 1. The blends were extruded and stored for further use.

Then, the blends were pressed in a hydraulic press as follows: 10 g of pellets were placed between two stainless steel plates and pressed at 110 °C. The pressing conditions were: 5 ton applied for five times, 5 ton for 5 min, and again 5 ton for 5 min [21].

2.2.3. Film conditioning and thickness

The films were conditioned at 23 ± 2 °C and $50 \pm 5\%$ RH for 48 h, before analysis [23]. The film thickness was measured by readings at

Table 1
Formulation of polymer blends subjected to extrusion.

Formulations	TPS (%)	TPP (%)	MPL (%)
P0L0	100	0	0
P25L0	75	25	0
P50L0	50	50	0
P75L0	25	75	0
P100L0	0	100	0
P0L4	100	0	4
P25L4	75	25	4
P50L4	50	50	4
P75L4	25	75	4
P100L4	0	100	4

15 different points, using a Mitutoyo digital micrometer (precision 0.01 mm; Mitutoyo Sul Americana, Suzano, SP, Brazil).

2.2.4. Scanning electron microscopy (SEM)

The morphology of the samples was analyzed by scanning electron microscopy (SEM), using the LEO EVO 40 XVP microscope (Zeiss, Cambridge, England), with an acceleration voltage of 15 kV. For that, the samples (2 mm \times 2 mm) were mounted on aluminum stubs for surface and cross-section observation, using double-coated carbon, and coated by gold plating under vacuum metallization.

2.2.5. Fourier transform infrared spectroscopy (FTIR)

The functional groups present in the samples were determined by Fourier transform infrared spectroscopy (FTIR). The FTIR analyses were performed on the Spectrometer Varian 600-IR Series (California, United States) with coupled Gladi ATR accessory from PIKE technologies and a diamond crystal. The spectral range was 4000 to 400 cm^{-1} with 256 scans and 4 cm^{-1} resolution.

2.2.6. Thermogravimetric analysis (TGA)

The thermal stability of the films was determined by thermogravimetric analysis (TGA) in the DTG60H-SHIMADZU apparatus (Kyoto, Japan). The analysis was performed under a nitrogen atmosphere at a flow rate of 50 mL/min, heating from 50 to 600 °C at a rate of 10 °C/min.

2.2.7. Mechanical properties

A TA-XT2 texture analyzer (Stable Micro Systems, England), with a 1 kN load cell was used for the perforation and tensile strength tests. For the perforation test, the thickness was measured in the samples (3 \times 3 cm) at four different points, which was fixed in metal support with a guide hole perforated perpendicularly to the plane of the plate. The test conditions were: 5.0 mm spherical probe (A/TG), speed of 0.8 mm/s, and gage length of 1 cm after touching the sample. Fifteen specimens were analyzed for each treatment [24]. The resistance to perforation/thickness (RP, N/mm) was calculated by dividing the maximum force at the breaking point by the film thickness to eliminate the effect of thickness variations. Deformation (D, mm) was determined through the breaking point of the specimens. For the tensile strength test, the film thickness (10 \times 1.5 cm) was determined at three different points and fixed on the probe support by the two ends. The test conditions were: 50 mm separation between clamping claws and speed of 0.8 mm/s. Fifteen specimens were analyzed for each treatment [25]. The maximum tensile strength (TS, MPa) was calculated by dividing the maximum force by the transverse area of the specimen. The percentage of elongation at break (EAB) was calculated by the ratio between increased length and initial length after breakage of the tested specimen. For the modulus of elasticity (ME, MPa) a tangent to the stress-strain curve in the linear region (elastic region) was plotted, and the ratio between the stress and the corresponding strain was calculated [26].

2.2.8. Water solubility

The water solubility of the films was determined through the percentage of soluble matter, according to Gontard and Guilbert [27], with modifications. The films (3 × 3 cm) were dried in a drying oven for 24 h at 105 °C, with subsequent cooling and weighing. Then, they were immersed in 50 mL of distilled water and stirred at 100 rpm, at 25 °C for 24 h. After this period, the films were dried under the same conditions and weighed. The water solubility was calculated according to Eq. (1).

$$\text{Solubility (\%)} = ((M_{\text{initial}} - M_{\text{final}}) / M_{\text{initial}}) \times 100 \quad (1)$$

where: M_{initial} is the mass (g) of the sample at the beginning of the analysis, and M_{final} is the mass (g) at the end of the analysis.

2.2.9. Water vapor permeability (WVP)

The water vapor permeability was determined by the gravimetric method. The films (1 cm in diameter) were sealed in permeation cells containing silica gel. The cells were placed in a desiccator with a saturated sodium chloride solution (NaCl) at 75 ± 3% RH and 23 ± 1 °C. Then, the samples were weighed over time (8-hour intervals) for 5 days to determine the weight gain related to the transfer of water vapor through the film [28]. The water vapor transmission rate and the water vapor permeability were calculated according to Eqs. (2) and (3), respectively.

$$\text{WVTR} = G/t \cdot A \quad (2)$$

where: WVTR is the water vapor transmission rate (g/m²·day); G/t is the slope of each line (g/day), and A is the permeation area of the specimen (m²).

$$\text{WVP} = \text{WVTR} \cdot e / \rho s (RH_1 - RH_2) \quad (3)$$

where: WVP is water vapor permeability (g m⁻¹ s⁻¹ Pa⁻¹); WVTR is the water vapor transmission rate; e is the film thickness (μm); ρs the saturation water vapor pressure at the test temperature (2800 kPa); RH_1 is the relative humidity of the chamber, and RH_2 is the relative humidity inside the cell.

2.2.10. Oxygen permeability (PO₂)

Four blends with the best results for thermal stability (TG/DTG), mechanical properties, solubility, and WVP were selected, two of them with the addition of MPL and two without MPL. The oxygen transmission rate of the films was measured on a Mocon Oxtran 1/50 (Minnesota - USA), at 50% RH, 23 °C, and 1 atm of partial oxygen pressure gradient. The oxygen permeability (PO₂) (cm³ mm m⁻² day⁻¹ atm¹) was calculated by multiplying the oxygen transmission rate by the film thickness. The determinations were performed in duplicate [29].

2.2.11. Antioxidant activity

The antioxidant potential of the films was determined by the 2,2-diphenyl-1-picryl-hydrazyl (DPPH) free radical capture method. For that, 0.2 g of sample was mixed with 2 mL of 80% methanol. The mixture was vortexed for 3 min and allowed to stand at room temperature for 3 h. Then, the mixture was vortexed for 3 min. An aliquot of the methanolic extract was mixed with 3.9 mL of 0.1 mM DPPH in 80% methanol. The mixture was vortexed for 1 min and allowed to stand in the dark for 30 min and 60 min. Absorbance readings were performed in a spectrometer (SP 2000UV, Monza, Italy) at 517 nm using 0.1 mM DPPH in 80% methanol as a control. The radical scavenging activity was calculated according to Eq. (3) [30]:

$$\text{RSA (\%)} = ((A_{\text{sample}} - A_{\text{control}}) / A_{\text{control}}) \times 100 \quad (4)$$

where:

A_{control} : Absorbance of the DPPH solution without the sample

A_{sample} : Absorbance of the sample with DPPH.

2.2.12. Optical properties

The color parameters L^* , a^* , and b^* were determined in a CM-700 colorimeter (Kônica Minolta, Japan), with D65 illuminant, observation angle of 10°, and specular reflectance included mode (SCI). The measurements were performed with the films superimposed on white-colored paper. The saturation index (C^*) was calculated according to the equation $C^* = [(a^{*2} + b^{*2})^{1/2}]$.

The transparency of the films was determined by measuring the transmittance percentage (%T) at 600 nm, using a spectrophotometer (Bel Spectro S-2000; Monza, Italy), according to ASTM D1746-03 [31]. The films (3 × 1 cm) were fixed to allow the beam to pass through the specimens without any obstacle. Transparency (T) was calculated according to Eq. (5):

$$T = (\text{Log}\%T) / \delta \quad (5)$$

where, T is the transparency of the film, and δ is the film thickness (mm).

The UV light absorption capacity of the films was determined in an S-2000 spectrophotometer (Bel Spectro, Monza, Italy) at 280 nm, 320 nm, 400 nm, 600 nm, and 800 nm.

2.2.13. Statistical analysis

The experiment was carried out in a completely randomized design (CRD) with three repetitions. The results of the thickness (mm), solubility (%), RP (MPa), D (mm), TS (MPa), EAB (%), ME (MPa), WVP (g m⁻¹ s⁻¹ Pa⁻¹), PO₂ (cm³ mm m⁻² day⁻¹ atm¹), optical properties, and antioxidant activity were subjected to analysis of variance (ANOVA) using the SISVAR software [32], at $p < 0.05$, and means were compared by Tukey's test. The results of SEM, FTIR, and TGA, were subjected to the descriptive analysis.

3. Results

3.1. Scanning electron microscopy (SEM)

The surface micrographs of the blends without MPL exhibited a homogeneous, compact structure, without the presence of pores, with some points of non-plasticized starch or starch molecules that underwent retrogradation, which decreased with the increase in the thermoplastic pectin concentration. These characteristics were maintained with the incorporation of MPL. However, non-dispersed MPL was found in the formulations containing higher thermoplastic starch concentrations (POL4 and P25L4), which reduced with increasing the concentration of thermoplastic pectin.

Probably, the presence of non-dispersed MPL in the blends containing higher thermoplastic starch concentrations was due to the different polarity of the polymers. Starch contains oxygen carbon and oxygen-hydrogen bonds, making it a polar molecule, while pectin has polar and nonpolar molecules, and Kraft lignin is nonpolar according to pH. Therefore, lignin interacts with the nonpolar groups of pectin by covalent and hydrogen bonds, forming more uniform films. In contrast, starch partially interacts with lignin, due to the difference in polarity, through hydrogen bonds between the functional groups of the molecules [10,19].

In addition to the better affinity between pectin and lignin, the greater uniformity of the blends containing higher TPP concentrations may be due to the lower viscosity of pectin, which dragged the MPL through the extruder, thus providing a better MPL dispersion [19].

It is known that starch and pectin have strong interfacial adhesion, due to the similarity of their structures, as both are polysaccharides, making miscible blends [12,33].

Irregular surfaces such as protrusion and roughness were observed mainly in the cross-sectional area due to the fracture region of the blends and the thermopressing. In addition, phase segregation may have occurred during the manufacturing process, once the plasticized

polymer pellets were obtained separately, for later preparation of the blends. Consequently, during extrusion, the low-viscosity pellets (TPP) flowed more quickly in the extruder, with little contact with the high-viscosity polymer (TPS) thus leading to the phase separation. This behavior is shown in Fig. 2, in which the lighter and more transparent regions refer to the starch molecules, while the dark brown regions refer to pectin, and the light brown refers to the mixture of both polymers [12].

3.2. Fourier transform infrared spectroscopy (FTIR)

Infrared spectroscopy was used to determine the possible interactions between TPS, TPP, and MPL of the polymeric blends.

Fig. 3 shows similar spectra between the polymer structures, with bands observed at 3287 cm^{-1} (OH stretching vibrations), 2924 cm^{-1} (CH stretching of stearic acid and methylene groups, and methyl group of the pectin chains), 1649 cm^{-1} (hydrogen bonds), and 925 cm^{-1} and 1149 cm^{-1} (α 1,4 glycosidic bonds). Other common bands were observed at 1076 cm^{-1} (C–O–C stretching vibrations of the saccharide structure, glucopyranose ring), 1016 cm^{-1} (C–OH stretching), 1410 cm^{-1} (characteristic of glycerol) and 1739 cm^{-1} and 1201 cm^{-1} corresponding to stearic and citric acids and ester linkages of pectin [10,34–39].

The spectrum of the lignin microparticles showed characteristic bands of this macromolecule at 1599 cm^{-1} , 1516 cm^{-1} , and 1419 cm^{-1} corresponding to C–C vibrations of the aromatic rings. The bands located at 1319 cm^{-1} , 1206 cm^{-1} , and 1110 cm^{-1} were related to the vibrations of the syringyl and guaiacyl rings. The band at 1027 cm^{-1} referred to the guaiacyl units, and the band at 824 cm^{-1} corresponded to the C–H vibration of aromatic rings [22,40,41].

A slight change in the band intensity was observed at 1725 cm^{-1} , and 1201 cm^{-1} corresponding to the pectin ester groups, probably due to the different concentration of this component in the blends [34,38]. Aromatic compounds from MPL were observed in the blends, evidenced by the appearance of a peak at 1519 cm^{-1} , which was more pronounced in the blends POL4, P50L4, and P100L4, due to the presence of aromatic rings from lignin [10].

3.3. Thermogravimetric analysis (TGA)

Thermogravimetric analysis is essential to assess the degradation temperature of the samples, and whether they are heat sensitive or heat resistant.

The DTG plot (Fig. 4C) shows that the films made with pure TPS (POL0) and pure TPP (P100L0) exhibited three degradation peaks, whereas the blends showed four degradation stages. For all formulations, the first stage was related to the evaporation event and water loss (from $50\text{ }^{\circ}\text{C}$ to $120\text{ }^{\circ}\text{C}$). The films made with pure TPS (POL0), and TPS + MPL (POL4) presented two more degradation stages, which is characteristic of thermoplastic starch and lignin, as follows: (II) $120\text{ }^{\circ}\text{C}/255\text{ }^{\circ}\text{C}$ elimination of glycerol and decomposition of hemicelluloses from MPL, with mass loss of 15.86% and 10.8%; (III) $300\text{ }^{\circ}\text{C}/350\text{ }^{\circ}\text{C}$ starch and lignin degradation, with 50.51% and 51.10% of mass loss [10,42,43].

As expected, the films made with TPP (P100L0) and TPP + MPL (P100L4) presented two more degradation stages. The first stage referred to the glycerol degradation at $160\text{ }^{\circ}\text{C}$, with mass loss of 15.21% and 25.14%, and the pectin degradation at $240\text{ }^{\circ}\text{C}$, with mass loss of 37.54% and 43.08%, respectively [11,38]. The TPP-based film showed lower thermal stability when compared to the TPS-based film (POL0), once maximum peak temperatures of $224\text{ }^{\circ}\text{C}$ and $312\text{ }^{\circ}\text{C}$ were observed for the formulations P100L0 and POL0, respectively.

This is mainly due to the difference in the molecular structure of the polymers. In the structure of pectin, there is the presence of carboxylate groups (COO⁻) that promote greater degradation reactions in which it is induced by several inter and intramolecular hydrogen bonds. [12,44].

When analyzing the blends with and without the incorporation of MPL, a characteristic behavior was observed for both polymers, which showed that the blends were immiscible, once only one peak overlap was observed (Fig. 4D), as previously reported by Moreira et al. [12].

There was an increase in *Tonset* in blends with 25% and 50% TPP when compared to the formulation made with 100% TPS. However, the blends containing a higher TPP concentration (75%) showed a reduction in *Tonset*. The addition of MPL did not change this parameter, except for the concentration of 75% (P75L4), which showed a reduction in temperature.

The maximum degradation temperature (*Tmax*) decreased with the incorporation of TPP, which indicates a slight interaction between the polymers, which changed de degradation temperature in the polymeric matrix TPS [12]. However, when the lignin microparticles were added, an increase in the maximum degradation temperature of the blends P25L4, P50L4 and P75L4 was observed due to the presence of aromatic compounds from MPL, thus improving their thermal stability (Table 2) [10,45].

The incorporation of thermoplastic pectin to the thermoplastic starch film gradually reduced the mass loss between the blends at the end of the analysis, as shown in Table 2. The addition of the lignin microparticles led to a decrease in mass loss of the TPS (POL0) and TPP (P100L0) films. However, the blends with higher TPP contents (P50L0 and P75L0) presented a reduction of mass loss at the end of the degradation process. In contrast, no changes were observed for the blend P25L0 with the incorporation of the microparticles.

Zhang et al. [15] reported an improvement in the thermal stability of TPS based films containing up to 15% lignin, with maximum temperature values from $297\text{ }^{\circ}\text{C}$ to $316\text{ }^{\circ}\text{C}$ due to the presence of phenolic compounds and the hydrophobicity of lignin. An improvement in thermal stability was observed for the blends with 25% and 50% TPP due to their better compatibility with MPL, in which the nonpolar fraction of TPP interacts with MPL that is nonpolar [33,46,47].

Aqil et al. [10] and Çalgeris et al. [45] reported that the improvement in the thermal stability of the films is due to the stability of the aromatic structure of lignin at high temperatures. In addition, lignin interacted with at least one of the polymers, leading to the formation of a cross-linking network, mainly with TPP, as observed in the SEM images (Fig. 1).

3.4. Mechanical properties

The mechanical properties allow evaluating the application of biodegradable and active films. These properties determine the resistance of the films to protect a certain amount of food and to guarantee ease of transport, handling, and storage.

As shown in Table 3, the incorporation of TPP into the TPS-based film increased the maximum tensile strength (TS) and modulus of elasticity (ME) and reduced the elongation at break (EAB) and deformation (D). A reduction in resistance to perforation (RP) was observed, and the lowest

Table 2
Thermogravimetric analysis of films.

Sample	T onset ($^{\circ}\text{C}$) ^a	T max ($^{\circ}\text{C}$) ^b	Weight loss 600 $^{\circ}\text{C}$ (%)
POL0	195	312	87,46
P25L0	249	308	79,42
P50L0	266	306	77,3
P75L0	192	306	74,72
P100L0	184	224	77,69
POL4	197	312	86,09
P25L4	249	312	79,43
P50L4	267	309	79,3
P75L4	189	308	75,9
P100L4	191	226	76,84

^a Temperature of onset of the maximum peak of degradation.

^b Maximum degradation temperature.

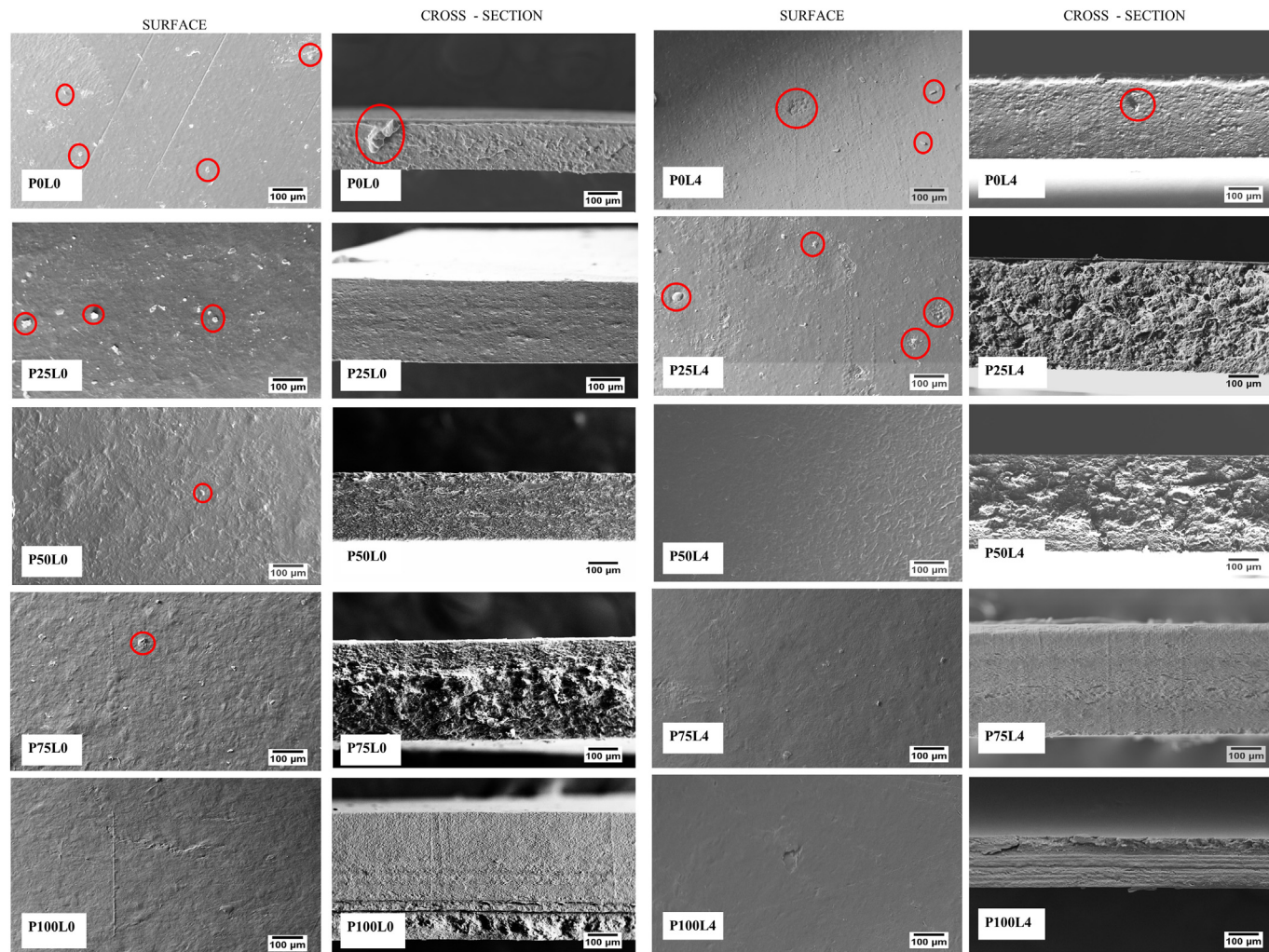


Fig. 1. SEM micrographs of the films obtained by extrusion: (I) films P0L0 (100% TPS), P25L0 (75% TPS/25% TPP), P50L0 (50% TPS/50% TPP), P75L0 (25% TPS/75% TPP), P100L0 (100% TPP), P0L4 (100% TPS/4% MPL), P25L4 (75% TPS/25% TPP/4% MPL), P50L4 (50% TPS/50% TPP/4% MPL), P75L4 (25% TPS/75% TPP/4% MPL), P100L4 (100% TPP/4% MPL).

value was observed for the blends with higher TPP concentrations. A similar result was observed for the blends with MPL. These results indicate that the incorporation of TPP conferred a greater rigidity with lower deformation, making the films more fragile.

The incorporation of MPL changed some properties of the films. The blend P25L4 presented increased EAB and D, that is, the film exhibited a greater deformation, becoming less fragile. In the P50L4 blend, there was a reduction in EAB, that is, it exhibited low elasticity. Concerning the TPS-based films (P0L4), a reduction in RP was observed, which became less resistant due to the incompatibility between starch and the lignin polymers, generating imperfections (Fig. 1). For the TPP-based

film (P100L4), there was a reduction in TS and RP, and an increase in ME, that is, the film presented lower ductility and higher rigidity. This improvement observed for the TPP-based films is mainly due to the greater interactions between this polymer and MPL. For the other properties and other blends, no significant differences were observed between the films with and without the addition of MPL.

Moreira et al. [12] evaluated different proportions of high and low methoxyl pectin and glycerol, and also observed that the higher TPS concentration conferred lower rigidity when compared to the blends containing higher TPP concentration. This behavior is shown by the lower ME and TS, and higher EAB values of the blends with higher TPS

Table 3
Mechanical properties of films.

Sample	TS (MPa)	ME (MPa)	EAB (%)	RP (N/mm)	D (mm)
P0L0	0,53 ± 0,17 ^a	0,004 ± 0,001 ^a	83,54 ± 2,47 ^c	22,62 ± 2,62 ^{bc}	5,72 ± 0,47 ^{de}
P25L0	1,26 ± 0,16 ^{bc}	0,031 ± 0,004 ^{ab}	24,97 ± 0,70 ^{bc}	33,01 ± 1,67 ^d	3,65 ± 0,33 ^c
P50L0	0,99 ± 0,25 ^{abc}	0,027 ± 0,08 ^{ab}	30,72 ± 6,21 ^c	22,07 ± 0,58 ^{bc}	3,63 ± 0,29 ^c
P75L0	1,42 ± 0,23 ^{bcd}	0,139 ± 0,013 ^c	8,23 ± 2,83 ^a	18,15 ± 1,90 ^{abc}	2,55 ± 0,13 ^{ab}
P100L0	3,57 ± 0,38 ^e	0,236 ± 0,027 ^d	10,77 ± 1,15 ^a	31,28 ± 4,26 ^d	2,48 ± 0,22 ^{ab}
P0L4	0,49 ± 0,13 ^a	0,004 ± 0,001 ^a	91,21 ± 4,87 ^e	13,48 ± 0,46 ^a	6,34 ± 0,04 ^e
P25L4	1,47 ± 0,21 ^{cd}	0,021 ± 0,006 ^{ab}	43,88 ± 9,48 ^d	32,71 ± 2,34 ^d	4,90 ± 0,05 ^d
P50L4	0,80 ± 0,03 ^{ab}	0,054 ± 0,003 ^{ab}	16,21 ± 2,45 ^{ab}	22,09 ± 2,11 ^{bc}	3,56 ± 0,19 ^c
P75L4	1,33 ± 0,21 ^{bcd}	0,085 ± 0,019 ^{bc}	13,72 ± 1,79 ^{ab}	26,46 ± 2,09 ^{cd}	3,25 ± 0,10 ^{bc}
P100L4	2,02 ± 0,25 ^d	0,460 ± 0,058 ^e	4,83 ± 0,56 ^a	16,77 ± 2,53 ^{ab}	2,08 ± 0,18 ^a

Means followed by equal letters in the column do not differ statistically from each other, by the Tukey's test ($p < 0.05$).

Table 4

Solubility analysis, water vapor permeability, film thickness and the oxygen permeability rate and coefficient at 23 °C/50% RH and 1 atm of partial oxygen pressure gradient.

Sample	Solubility (%)	PVA ($\text{g} \cdot \text{m}^{-1} \cdot \text{s}^{-1} \cdot \text{Pa}^{-1}$) $\times 10^{13}$	Thickness (mm)	PO ₂ ($\text{cm}^3 \text{ mm}^{-2} \text{ dia}^{-1} \text{ atm}^{-1}$)
P0L0	0,59 ± 0,16 ^{ab}	5,58 ± 0,53 ^a	0,43 ± 0,04 ^{bc}	–
P25L0	0,47 ± 0,05 ^{ab}	7,07 ± 0,29 ^{ab}	0,35 ± 0,01 ^{ab}	1,65 ± 0,04 ^a
P50L0	0,46 ± 0,08 ^{ab}	9,01 ± 1,39 ^{bc}	0,33 ± 0,02 ^a	1,95 ± 0,15 ^a
P75L0	0,41 ± 0,04 ^{ab}	8,65 ± 0,45 ^{bc}	0,42 ± 0,02 ^{bc}	–
P100L0	0,67 ± 0,10 ^b	13,73 ± 0,48 ^d	0,51 ± 0,02 ^c	–
P0L4	0,37 ± 0,11 ^a	10,42 ± 1,51 ^c	0,46 ± 0,01 ^{cd}	–
P25L4	0,34 ± 0,12 ^a	9,08 ± 0,52 ^{bc}	0,42 ± 0,02 ^{bc}	0,85 ± 0,02 ^b
P50L4	0,33 ± 0,10 ^a	10,79 ± 0,49 ^c	0,35 ± 0,02 ^{ab}	0,68 ± 0,21 ^b
P75L4	0,45 ± 0,04 ^{ab}	8,61 ± 0,67 ^{bc}	0,42 ± 0,02 ^{bc}	–
P100L4	0,43 ± 0,09 ^{ab}	8,67 ± 0,86 ^{bc}	0,45 ± 0,02 ^{cd}	–

Means followed by equal letters in the column do not differ statistically from each other, by the Tukey's test ($p < 0.05$).

concentration, due to the presence of amylopectin molecules, which has a branched and more flexible structure than amylose, thus promoting a film with greater ductility.

3.5. Thickness, solubility, WVP, and PO₂

The film thickness as well as interactions and arrangements can affect the solubility, and the permeability to water vapor and oxygen. Thinner films tend to have more hydrogen bonds and other chemical interactions [48].

No changes were observed in the film thickness in the present study for the polymer blends containing different TPS/TPP concentrations. However, a slight increase in thickness was observed for the formulations P0L4, P25L4, and P50L4 with the addition of MPL, probably due to the weak interactions between MPL and TPS. The formulation P100L4 had a decrease in thickness, that is, the thermoplastic pectin had stronger interactions with MPL when compared to TPS (Table 4). These results corroborate with those found in scanning electron microscopy (Fig. 1) and FTIR (Fig. 3).

The determination of solubility allows assessing the solubility of the material in an aqueous medium for a given time. The results indicate whether the film can be used for foods with high water activity and high moisture, which requires poorly water soluble films.

No difference was observed in the solubility of TPS/TPP-based films with and without the addition of MPL. However, for all treatments, the pure TPP film (P100L0) was more soluble than the films P0L4, P25L4, and P50L4, which contained TPS in the formulations. The blends with higher TPS contents (P25L4 and P50L4) showed lower solubility (27%) due to the presence of MPL, while the blend with the highest TPP concentration (P75L4) showed an increase in solubility of approximately 9%. Kraft lignin is hydrophobic, which impairs the water absorption in the films [10].

The WVP of films is an important parameter, as it determines the ability of a film to absorb water from the atmosphere into food. Increased water absorption can accelerate the deterioration and contribute to microbial growth [49,50].

No significant effect was observed for the WVP between the films with MPL, while differences were observed for the films without the addition of MPL, with a higher WVP value for the treatment P100L0. The films P75L0, P50L0, and P25L0 also presented higher values when compared with P0L0 (Table 4), showing that the addition of TPP to the starch-based films increased the water vapor permeability.

This behavior is due to the presence of OH groups and high methoxyl pectin, which have an affinity for water. Probably, the combination with starch led to the formation of hydrogel complexes, resulting in greater hydrophilicity [1].

When comparing all treatments, the film with 100% TPS (P0L0) showed higher WVP with the incorporation of MPL (P0L4). On the other hand, the film with 100% TPP (P100L0) showed a decrease in permeability with the addition of MPL (P100L4) (Table 4). This behavior is probably due to the greater affinity between pectin and lignin microparticles, as shown by scanning electron microscopy (Fig. 1), thus filling the

empty spaces in TPP, and impairing the permeate (water) to pass through the film. In contrast, little interaction of the thermoplastic starch (TPS) was observed for the film made with 100% TPS and addition of MPL, due to differences in polarity, leading to imperfections between the starch molecules and the lignin microparticles.

In the analysis of water solubility, the polymer is immersed in water, therefore, all molecules present in the polymeric matrix will come into contact with water [51]. In the WVP analysis, water vapor is transported by the polymer, where three mechanisms occur: absorption of water vapor on the film surface, diffusion of water vapor through the film and, finally, water vapor desorption, on the surface of the film [52]. Therefore, the decrease in solubility values in the films after the addition of MPL probably occurred due to the presence of hydrophobic particles in the blends, protecting the films from water absorption [10]. Likewise, the addition of MPL promoted an increase in the rate of permeability to water, probably due to the weak interaction of MPL with polymers, which may have facilitated the diffusion and desorption of the water molecule in the polymeric network [20].

The incorporation of MPL into the polymeric blends reduced the rate and the coefficient of oxygen permeability, proving its efficiency as antioxidant agents.

The reduction in oxygen permeability values is directly related to the presence of lignin microparticles in the films. In addition, MPL led to an increase in tortuosity associated with the crosslinking effect, with the formation of a three-dimensional network by covalent bonds, preventing mass transport [29,53]. The phenolic groups from lignin also acted as antioxidant agents, presenting greater activity at higher concentrations, as shown in Table 5.

3.6. Antioxidant activity

The antioxidant activity is essential to evaluate the quality of the active film for use in foods susceptible to lipid oxidation, which impairs the food quality by changing the sensory characteristics. The analysis of

Table 5

Antioxidant analysis of TPS/TPP films without and with MPL obtained by extrusion.

Films	RSA (%)	
	30 min	60 min
P0L0	2,61 ± 0,98 ^a	2,83 ± 1,77 ^a
P25L0	2,8 ± 0,53 ^a	2,72 ± 0,49 ^a
P50L0	4,12 ± 0,35 ^a	4,12 ± 0,28 ^a
P75L0	4,61 ± 0,14 ^a	4,69 ± 0,19 ^a
P100L0	8,69 ± 0,38 ^b	8,96 ± 0,51 ^b
P0L4	66,83 ± 1,32 ^c	71,52 ± 1,33 ^c
P25L4	66,51 ± 1,83 ^c	71,08 ± 1,86 ^c
P50L4	75,89 ± 1,57 ^d	79,28 ± 0,83 ^d
P75L4	80,03 ± 0,37 ^e	82,42 ± 0,22 ^{de}
P100L4	81,27 ± 0,61 ^e	83,29 ± 0,64 ^e

Means followed by equal letters in the column do not differ statistically from each other, by the Tukey's test ($p < 0.05$).

Table 6
Color analysis of films obtained by extrusion.

Sample	L	a	b	C*	h°
P0L0	85,55 ± 1,12 ^c	−0,7 ± 0,13 ^a	3,18 ± 1,42 ^a	3,28 ± 1,38 ^a	104,96 ± 7,43 ^b
P25L0	77,18 ± 2,02 ^c	1,85 ± 0,92 ^{ab}	19,87 ± 2,12 ^b	19,97 ± 2,19 ^b	84,90 ± 2,11 ^{ab}
P50L0	76,25 ± 1,94 ^c	2,61 ± 1,17 ^b	20,88 ± 0,92 ^b	21,07 ± 0,96 ^b	82,92 ± 3,08 ^{ab}
P75L0	59,72 ± 1,72 ^b	10,48 ± 0,97 ^c	27,20 ± 5,46 ^c	29,23 ± 5,10 ^c	68,33 ± 4,13 ^{ab}
P100L0	52,16 ± 3,19 ^{ab}	12,53 ± 2,11 ^c	21,28 ± 6,17 ^{bc}	24,74 ± 6,34 ^{bc}	58,80 ± 3,54 ^a
P0L4	42,50 ± 6,78 ^a	0,77 ± 0,31 ^{ab}	1,45 ± 0,68 ^a	1,77 ± 0,36 ^a	57,41 ± 25,14 ^a
P25L4	40,30 ± 7,46 ^a	0,76 ± 0,50 ^{ab}	1,64 ± 0,55 ^a	1,94 ± 0,22 ^a	63,46 ± 22,42 ^a
P50L4	40,10 ± 7,76 ^a	1,48 ± 0,88 ^{ab}	2,36 ± 0,79 ^a	2,88 ± 0,93 ^a	60,01 ± 15,35 ^a
P75L4	40,08 ± 7,65 ^a	1,84 ± 0,83 ^{ab}	2,64 ± 0,37 ^a	3,31 ± 0,47 ^a	56,46 ± 13,11 ^a
P100L4	40,91 ± 7,0 ^a	1,14 ± 0,69 ^{ab}	2,73 ± 0,14 ^a	3,02 ± 0,31 ^a	68,30 ± 11,65 ^{ab}

Means followed by equal letters in the column do not differ statistically from each other, by the Tukey's test ($p < 0.05$).

antioxidant activity by DDPH assay showed low antioxidant activity of the TPS- and TPP-based films (Table 5).

The films with MPL (4%) exhibited higher antioxidant activity when compared to TPS/TPP films, mainly those containing higher TPP concentrations (P75L4 and P100L4). In addition, the time of exposure to the DPPH radical influenced the results, with higher values observed for the films containing lignin microparticles (Table 5).

These results are due to the presence of phenolic groups, hydroxyls, and double bonds in the structure of the lignin microparticle, which acted as an antioxidant agent in the polymeric blends. These functional groups act as free radical scavengers, donating hydrogen, and stopping the oxidation reactions, due to the stabilization of free radicals [7,19,53].

3.7. Optical properties

The addition of TPP provided a lower L* (luminosity), higher a* (red/green), b+ (yellow/blue) and C* (saturation) values, and lower h° (hue), while the addition of 4% MPL reduced all color parameters, due to the dark brown color of MPL.

The blends with TPS/TPP (P25L0, P50L0, and P75L0) presented positive a* (red), b* (yellow), and C* (saturation) values, which increased with increasing the TPP concentrations, while lower values were observed for the hue angle (h°).

When analyzing the films P0L0 to P100L0 (Table 6 and Fig. 2), the TPP changed the color of the films to a darker tone, from light beige to

yellowish-red and then brown. As expected, the TPS-based film (P0L0) showed a higher hue angle (h°), with a tendency for the blue color, due to the lighter color of starch when compared to pectin, which is white and light beige, respectively.

The TPP-based film showed a darker color than it was expected, probably due to the heat treatment during the production of the films, which led to non-enzymatic browning, known as caramelization. Some factors are responsible for darkening, including heat (temperature > 120 °C), pH values ($9 < \text{pH} < 3$), and time of exposure, which is catalyzed by the presence of acids. For the production of the films, citric acid (antioxidant agent) and stearic acid (anticaking agent) was used. Thus, both compounds may have contributed to the high temperature (extrusion and pressing) for the caramelization of pectin during thermopressing and production of the films [54–56].

No differences in color intensity and luminosity were observed for the films P0L4 to P100L4 (Table 6), which exhibited an opaque dark brown color. The incorporation of MPL into the films may have standardized the color, masking the color differences between the films P50L0 and P75L0 (Fig. 2).

Opacity (lower transparency rate) is a desirable parameter to decrease the passage of light in the packaging material used to protect photosensitive foods [57], and the lower the value, the greater the opacity of the film. Thus, the incorporation of MPL into the films increased opacity, thus reduced the transparency, regardless of the amount of thermoplastic starch and thermoplastic pectin used (Table 7). This

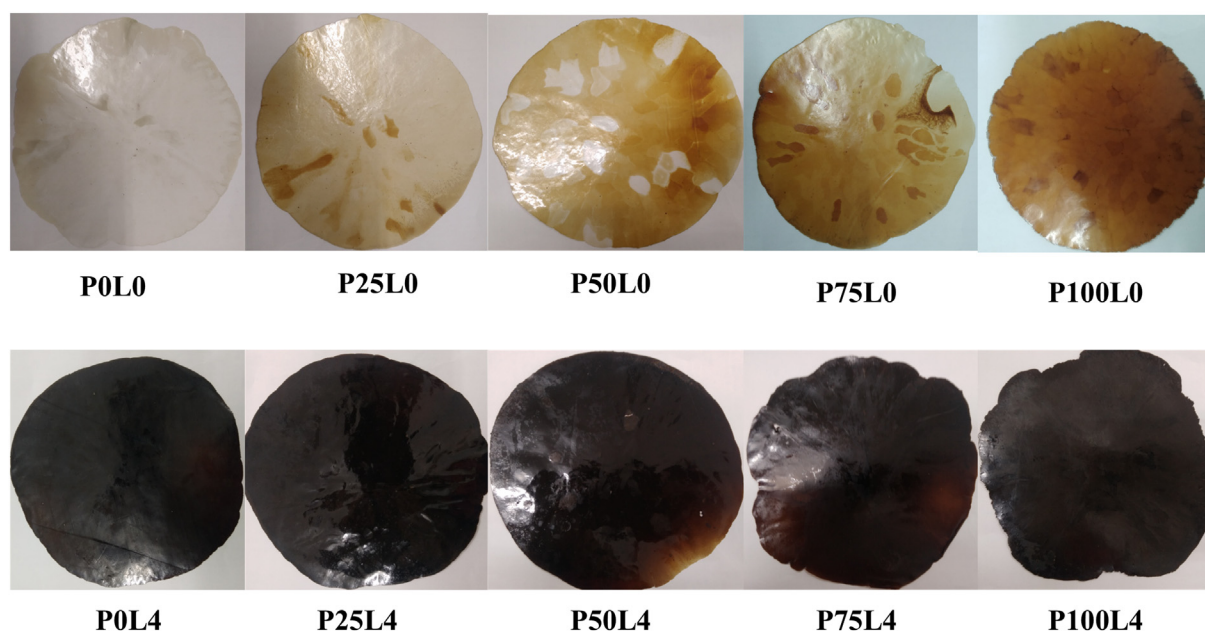


Fig. 2. Films obtained after the extrusion and pressing: P0L0 (100% TPS), P25L0 (75% TPS/25% TPP), P50L0 (50% TPS/50% TPP), P75L0 (25% TPS/75% TPP), P100L0 (100% TPP), P0L4 (100% TPS/4% MPL), P25L4 (75% TPS/25% TPP/4% MPL), P50L4 (50% TPS/50% TPP/4% MPL), P75L4 (25% TPS/75% TPP/4% MPL), P100L4 (100% TPP/4% MPL).

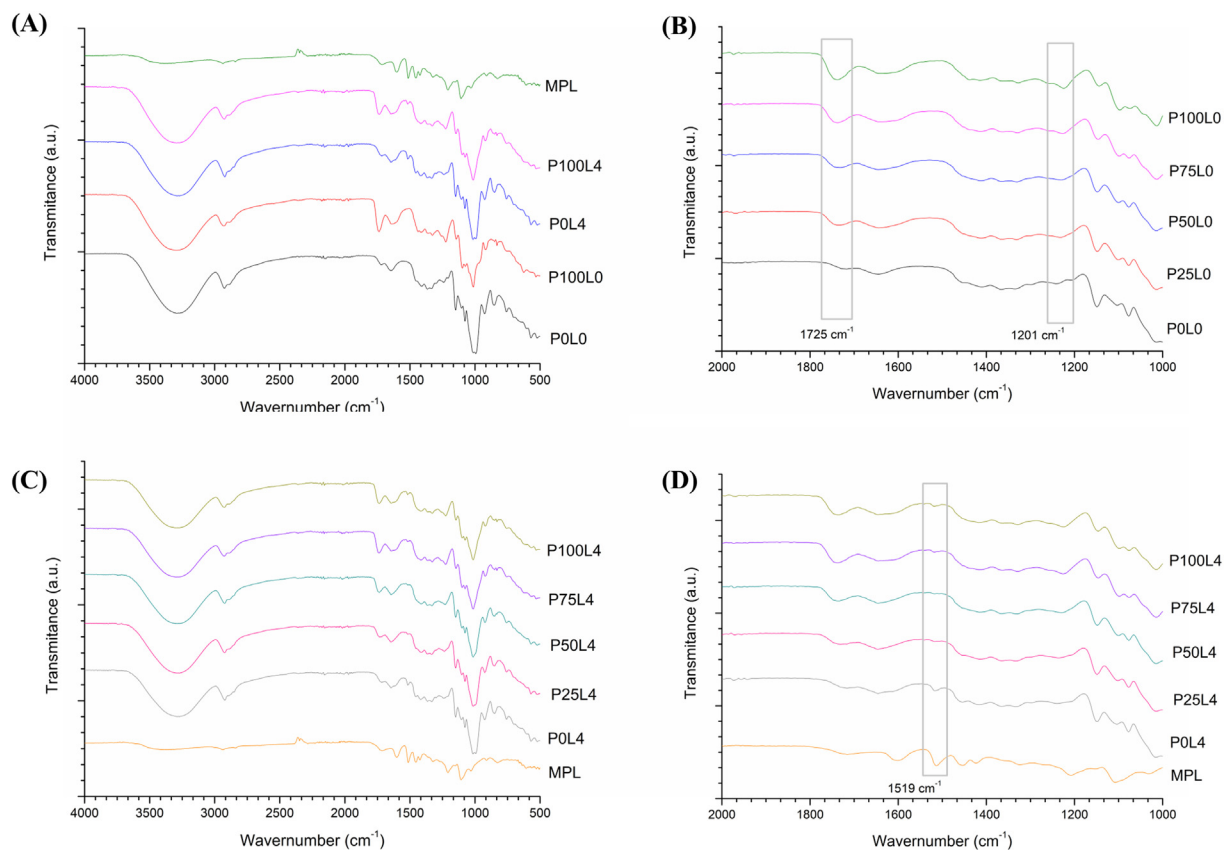


Fig. 3. FTIR spectrum of the TPS/TPP (A and B) and TPS/TPP/MPL (C and D) blends.

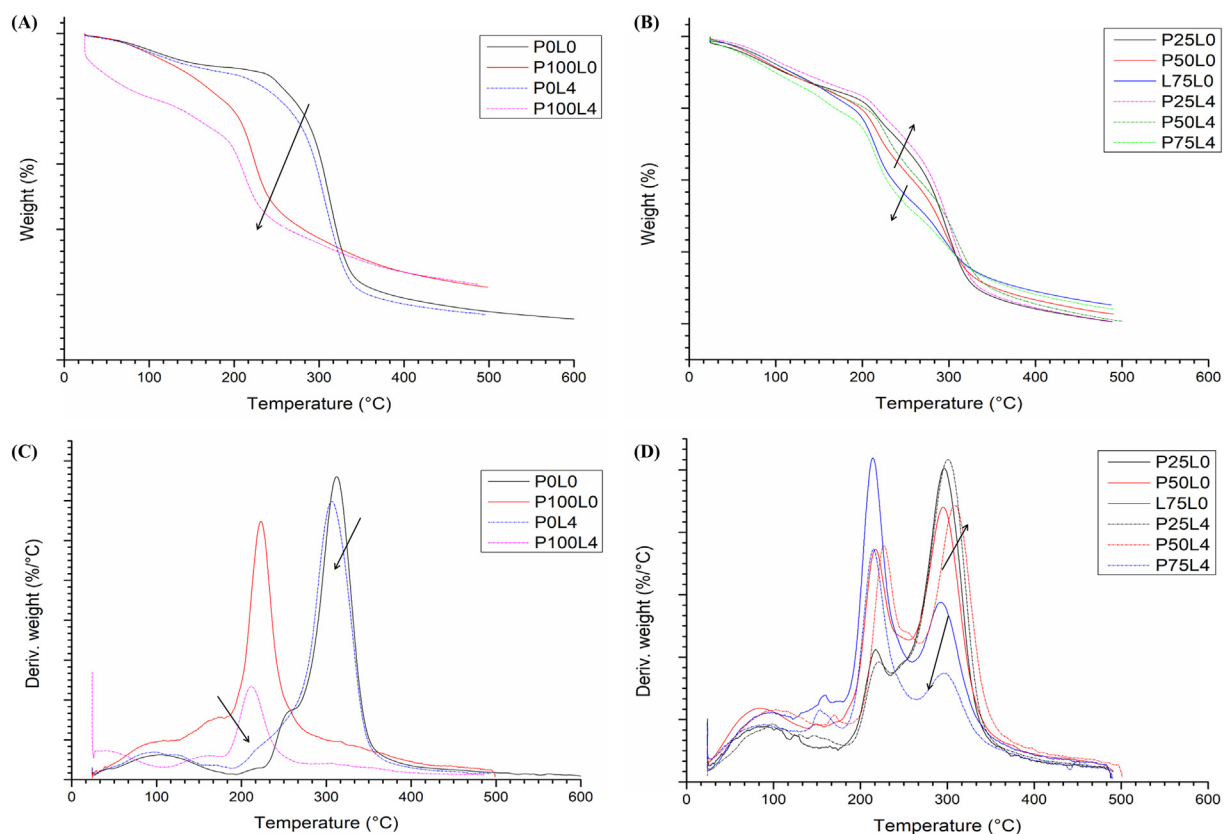


Fig. 4. Thermogravimetric curves of the films obtained by extrusion.

Table 7
Transmittance analysis (%) and opacity of films obtained by extrusion.

Sample	Transmittance (%)					T ₆₀₀
	280 nm	320 nm	400 nm	600 nm	800 nm	
P0L0	0,74 ± 0,75 ^a	2,89 ± 2,18 ^a	11,14 ± 5,17 ^a	19,37 ± 7,35 ^b	26,15 ± 8,63 ^b	3,24 ± 1,48 ^b
P25L0	0,00 ± 0,0 ^a	0,35 ± 0,25 ^b	11,62 ± 3,82 ^a	31,25 ± 3,35 ^{ab}	41,46 ± 2,61 ^{ab}	3,61 ± 0,20 ^{ab}
P50L0	0,00 ± 0,0 ^a	0,25 ± 0,33 ^b	9,03 ± 1,96 ^a	33,01 ± 1,36 ^a	45,39 ± 1,25 ^a	4,74 ± 0,19 ^a
P75L0	0,00 ± 0,0 ^a	0,00 ± 0,0 ^b	2,23 ± 0,68 ^b	27,75 ± 4,12 ^{ab}	44,49 ± 5,42 ^{ab}	3,59 ± 0,55 ^{ab}
P100L0	0,00 ± 0,0 ^a	0,00 ± 0,0 ^b	0,46 ± 0,23 ^b	29,75 ± 1,76 ^b	55,26 ± 1,66 ^b	2,82 ± 0,18 ^b
P0L4	0,01 ± 0,01 ^a	0,01 ± 0,03 ^b	0,00 ± 0,0 ^b	0,01 ± 0,01 ^c	0,14 ± 0,09 ^c	0,00 ± 0,0 ^c
P25L4	0,00 ± 0,0 ^a	0,00 ± 0,0 ^b	0,00 ± 0,0 ^b	0,01 ± 0,01 ^c	0,28 ± 0,21 ^c	0,00 ± 0,0 ^c
P50L4	0,00 ± 0,0 ^a	0,00 ± 0,0 ^b	0,00 ± 0,0 ^b	0,07 ± 0,09 ^c	1,93 ± 1,47 ^c	0,00 ± 0,0 ^c
P75L4	0,00 ± 0,0 ^a	0,00 ± 0,0 ^b	0,00 ± 0,0 ^b	0,00 ± 0,0 ^c	0,49 ± 0,69 ^c	0,00 ± 0,0 ^c
P100L4	0,00 ± 0,0 ^a	0,00 ± 0,0 ^b	0,00 ± 0,0 ^b	0,00 ± 0,0 ^c	0,22 ± 0,23 ^c	0,00 ± 0,0 ^c

Means followed by equal letters in the column do not differ statistically from each other, by the Tukey's test ($p < 0.05$).

result corroborates with the luminosity results, in which opaque materials do not transmit light, thus interconnecting with the decreased luminosity of the films with MPL. This behavior was expected due to the naturally dark coloring of the lignin microparticles.

According to Wang and Rhim [58], opacity is directly affected by both the crystallinity of the material and the compact structures of the polymer chains that hinder the light passage. Thus, the microparticles may have filled the empty spaces between the polymer chains, providing more compact films, thus promoting greater opacity of the blends.

A reduction in the transmission of UV light (280 nm, 320 nm, 400 nm) was observed in the blends made with thermoplastic pectin without the addition of MPL, due to its naturally darker color when compared with the thermoplastic starch (Table 6). As expected, the production of blends with the incorporation of lignin microparticles decreased and even blocked light transmission at all wavelengths evaluated, including ultraviolet light (280 nm and 320 nm), visible light (400 nm and 600 nm), and infrared region (800 nm) (Table 7).

4. Conclusion

The present study is a pioneer in the use of thermoplastic starch and thermoplastic pectin with the incorporation of lignin microparticles to produce polymeric films by extrusion for use in active packaging. Regarding the film properties, pectin increased the mechanical strength and UV protection of the blends. The films with 25% and 50% thermoplastic pectin containing the lignin microparticles showed greater thermal stability, and the blend exhibited better mechanical properties when compared to the reference standards. All blends with the incorporation of lignin microparticles presented an increase in UV protection, becoming more opaque, with a dark brown color. The blends P25L4 and P50L4 presented a lower oxygen permeability and good antioxidant capacity. Therefore, the formulation made with 25% thermoplastic pectin containing lignin microparticles has proven to be an effective alternative for use in foods sensitive to oxygen and UV light.

CRedit authorship contribution statement

Danielly de Oliveira Begali: Project administration, conceptualization, methodology, formal analysis, investigation, writing - original draft, writing - review & editing. **Laura Fonseca Ferreira:** Methodology, validation, investigation, formal analysis. **Ana Carolina Salgado de Oliveira:** Methodology, validation, investigation, formal analysis. **Soraia Vilela Borges:** Conceptualization, methodology, visualization, formal analysis, resources, supervision, funding acquisition. **Alfredo Rodrigues de Sena Neto:** Data curation, investigation, formal analysis, resources. **Cassiano Rodrigues de Oliveira:** Data curation, investigation, formal analysis, resources. **Maria Irene Yoshida:** Data curation, resources. **Claire Sarantópoulos:** Data curation, resources.

Acknowledgments

The authors thank the Foundation for Research Support of the State of Minas Gerais (FAPEMIG); the National Council for Scientific and Technological Development (CNPq); and the Coordination for the Improvement of Higher Education Personnel (CAPES) for financial support and scholarships. The authors also thank the Laboratory of Electron Microscopy and Analysis of Ultrastructural Federal University of Lavras, (<http://www.prp.ufla.br/labs/microscopiaeletronica/>) and Finep, Fapemig, CNPq and Capes for supplying the equipment and technical support for experiments involving electron microscopy. The authors would like to thank the Federal University of Viçosa (Rio Paranaíba Campus) for the provision of equipment and technical support for experiments.

References

- [1] A.L.D. Róz, P. Veiga-Santos, A.M. Ferreira, T.C.R. Antunes, F.L. Leite, F.M. Yamaji, A.J.F. Carvalho, Water susceptibility and mechanical properties of thermoplastic starch - pectin blends reactively extruded with edible citric acid, *Mater. Res.* 19 (2016) 138–142, <https://doi.org/10.1590/1980-5373-MR-2015-0215>.
- [2] C.L. Barizão, M.I. Crepaldi, O. de O. S. Junior, A.C. de Oliveira, A.F. Martins, P.S. Garcia, E.G. Bonafé, Biodegradable films based on commercial κ-carrageenan and cassava starch to achieve low production costs, *Int. J. Biol. Macromol.* 165 (2020) 582–590, <https://doi.org/10.1016/j.ijbiomac.2020.09.150>.
- [3] M.D. Eaton, D. Domene-López, Q. Wang, M.G. Montalbán, I. Martín-Gullón, K.R. Shull, Exploring the effect of humidity on thermoplastic starch films using the quartz crystal microbalance, *Carbohydr. Polym.* (2021) 117727, <https://doi.org/10.1016/j.carbpol.2021.117727>.
- [4] J. Meerasri, R. Sothornvit, Characterization of bioactive film from pectin incorporated with gamma-aminobutyric acid, *Int. J. Biol. Macromol.* 147 (2020) 1285–1293, <https://doi.org/10.1016/j.ijbiomac.2019.10.094>.
- [5] H.G.R. Younis, H.R.S. Abdellatif, F. Yea, G. Zhao, Tuning the physicochemical properties of apple pectin films by incorporating chitosan/pectin fiber, *Int. J. Biol. Macromol.* 159 (2020) 213–221, <https://doi.org/10.1016/j.ijbiomac.2020.05.060>.
- [6] R.A.C. Gomide, A.C.S. de Oliveira, D.A.C. Rodrigues, C.R. de Oliveira, O.B.G. Assis, M.V. Dias, S.V. Borges, Development and characterization of lignin microparticles for physical and antioxidant enhancement of biodegradable polymers, *J. Polym. Environ.* 28 (2020) 1326–1334, <https://doi.org/10.1007/s10924-020-01685-z>.
- [7] W. Yang, E. Fortunati, F. Dominici, G. Giovanale, A. Mazzaglia, G.M. Balestra, J.M. Kenny, D. Puglia, Effect of cellulose and lignin on disintegration, antimicrobial and antioxidant properties of PLA active films, *Int. J. Biol. Macromol.* 89 (2016) 360–368, <https://doi.org/10.1016/j.ijbiomac.2016.04.068>.
- [8] W. Yang, E. Fortunati, F. Dominici, G. Giovanale, A. Mazzaglia, G.M. Balestra, J.M. Kenny, D. Puglia, Synergic effect of cellulose and lignin nanostructures in PLA based systems for food antibacterial packaging, *Eur. Polym. J.* 79 (2016) 1–12, <https://doi.org/10.1016/j.eurpolymj.2016.04.003>.
- [9] P. Ortiz-Serna, M. Carsí, M. Culebras, M.N. Collins, M.J. Sanchis, Exploring the role of lignin structure in molecular dynamics of lignin/bio-derived thermoplastic elastomer polyurethane blends, *Int. J. Biol. Macromol.* 158 (2020) 1369–1379, <https://doi.org/10.1016/j.ijbiomac.2020.04.261>.
- [10] M. Aqil, A.M. Nzenguet, Y. Essamlali, A. Snik, M. Larzek, M. Zahouily, Graphene oxide filled lignin/starch polymer bionanocomposite: structural, physical, and mechanical studies, *J. Agric. Food Chem.* 65 (2017) 10571–10581, <https://doi.org/10.1021/acs.jafc.7b04155>.
- [11] A.B. Meneguini, B.S.F. Cury, A.M. Santos, D.F. Franco, H.S. Barud, E.C. Silva Filho, Resistant starch/pectin free-standing films reinforced with nanocellulose intended for colonic methotrexate release, *Carbohydr. Polym.* 157 (2017) 1013–1023, <https://doi.org/10.1016/j.carbpol.2016.10.062>.

- [12] F.K.V. Moreira, J.M. Marconcini, L.H.C. Mattoso, Analysis of the influence of composition and processing parameters on the mechanical properties of biodegradable starch/pectin blends, *Polym. Bull.* 69 (2012) 561–577, <https://doi.org/10.1007/s00289-012-0750-x>.
- [13] K.K. Dasha, N. Afzal Ali, D. Das, D. Mohanta, Thorough evaluation of sweet potato starch and lemon-waste pectin based-edible films with nano-titania inclusions for food packaging applications, *Int. J. Biol. Macromol.* 139 (2019) 449–458, <https://doi.org/10.1016/j.ijbiomac.2019.07.193>.
- [14] W.G. Sganzerla, G.B. Rosa, A.L.A. Ferreira, C.G. da Rosa, P.C. Beling, L.O. Xavier, C.M. Hansen, J.P. Ferrareze, M.R. Nunes, P.L.M. Barreto, A. Paulad, L. Veck, Bioactive food packaging based on starch, citric pectin and functionalized with *Acca sellowiana* waste by-product: characterization and application in the postharvest conservation of apple, *Int. J. Biol. Macromol.* 147 (2020) 295–303, <https://doi.org/10.1016/j.ijbiomac.2020.01.074>.
- [15] C.W. Zhang, S.S. Nair, H. Chen, N. Yan, R. Farnood, F. Li, Thermally stable, enhanced water barrier, high strength starch biocomposite reinforced with lignin containing cellulose nanofibrils, *Carbohydr. Polym.* 230 (2020), 115626, <https://doi.org/10.1016/j.carbpol.2019.115626>.
- [16] M.L. Fishman, D.R. Coffin, C.I. Onwulata, Extrusion of pectin/starch blends plasticized with glycerol, *Carbohydr. Polym.* 41 (2000) 17–325, [https://doi.org/10.1016/S0144-8617\(99\)00117-4](https://doi.org/10.1016/S0144-8617(99)00117-4).
- [17] M.L. Fishman, D.R. Coffin, C.I. Onwulata, R.P. Konstance, Extrusion of pectin and glycerol with various combinations of orange albedo and starch, *Carbohydr. Polym.* 57 (2004) 401–413, <https://doi.org/10.1016/j.carbpol.2004.05.014>.
- [18] S. Baumberger, C. Lapiere, B. Monties, G. Della Valle, Use of kraft lignin as filler for starch films, *Polym. Degrad. Stabil.* 59 (1997) 213–221, [https://doi.org/10.1016/S0141-3910\(97\)00193-6](https://doi.org/10.1016/S0141-3910(97)00193-6).
- [19] M.F. Borisenkov, A.P. Karmanov, L.S. Kocheva, P.A. Markov, E.I. Istomina, L.A. Bakutova, S.G. Litvintseva, E.A. Martinson, E.A. Durnev, F.V. Vityazev, S.V. Popov, Adsorption of β -glucuronidase and estrogens on pectin/lignin hydrogel particles, *Int. J. Polym. Mater.* 65 (2016) 433–441, <https://doi.org/10.1080/00914037.2015.1129955>.
- [20] L.F. Ferreira, A.C.S. de Oliveira, D.O. Begali, A.R.S. Neto, M.A. Martins, J.E. de Oliveira, S.V. Borges, M.I. Yoshida, G.H.D. Tonoli, M.V. Dias, Characterization of cassava starch/soy protein isolate blends obtained by extrusion and thermocompression, *Ind. Crop. Prod.* 160 (2021), 113092, <https://doi.org/10.1016/j.indcrop.2020.113092>.
- [21] V.M. Azevedo, S.V. Borges, J.M. Marconcini, M.I. Yoshida, A.R.S. Neto, T.C. Pereira, C.F.G. Pereira, Effect of replacement of corn starch by whey protein isolate in biodegradable film blends obtained by extrusion, *Carbohydr. Polym.* 157 (2017) 971–980, <https://doi.org/10.1016/j.carbpol.2016.10.046>.
- [22] A.C.S. de Oliveira, L.F. Ferreira, D.O. Begali, J.C. Ugucioni, A.R.S. Neto, M.I. Yoshida, S.V. Borges, Thermoplasticized pectin by extrusion/thermo-compression for film industrial application, *J. Polym. Environ.* (2021) <https://doi.org/10.1007/s10924-021-02054-0>.
- [23] ASTM, Standard Practice for Conditioning Plastics for Testing, D618–00, American Society Standard Testing and Materials, Philadelphia, 2000 (2000a. 4 p).
- [24] ASTM, Standard Test Method for Slow Rate Penetration Resistance of Flexible Barrier Films and Laminates, F1306–90, American Society Standard Testing and Materials, Philadelphia, 2001 (2001. 4 p).
- [25] ASTM, Standard Test Method for Tensile Properties of Thin Plastic Sheeting D882–02, 2002, American Society Standard Testing and Materials, Philadelphia, 2002 (10 p).
- [26] C.I.G.L. Sarantópoulos, F.G. Teixeira, Embalagens plásticas flexíveis: Principais polímeros e avaliação das propriedades, 2nd ed. CETEA/ITAL, Campinas, 2002 267.
- [27] N. Gontard, S. Guilbert, Bio-packaging: technology and properties of edible and/or biodegradable material of agricultural origin, in: M. Mathlouthi (Ed.), *Food Packag. Preserv.* Springer, Boston, MA 1994, pp. 159–181.
- [28] ASTM, Standard Test Method for Water Vapor Transmission of Materials E96–00, American Society Standard Testing and Materials, Philadelphia, 2000 (2000b. 9 p).
- [29] J. Bonilla, E. Talón, L. Atarés, M. Vargas, A. Chiralt, Effect of the incorporation of antioxidants on physicochemical and antioxidant properties of wheat starch–chitosan films, *J. Food Eng.* 118 (2013) 271–278, <https://doi.org/10.1016/j.jfoodeng.2013.04.008>.
- [30] H. Byun, Y.T. Kim, S. Whiteside, Characterization of an antioxidant polylactic acid (PLA) film prepared with α -tocopherol, BHT and polyethylene glycol using film cast extruder, *J. Food Eng.* 100 (2010) 239–244, <https://doi.org/10.1016/j.jfoodeng.2010.04.005>.
- [31] ASTM, Standard Test Method for Transparency of Plastic Sheeting D1746–03, American Society Standard Testing and Materials, Philadelphia, 2003.
- [32] D.F. Ferreira, SISVAR: um programa para análises e ensino de estatística, *Ver. Cient. Symposium 6* (2) (2008) 36–41.
- [33] M.H.G. Canteri, L. Moreno, G. Wosiacki, A.P. Scheer, Pectina: da matéria-prima ao produto final, *Polim 22* (2012) 149–157, <https://doi.org/10.1590/S0104-14282012005000024>.
- [34] P. Ezati, J.H. Rhim, pH-responsive pectin-based multifunctional films incorporated with curcumin and sulfur nanoparticles, *Carbohydr. Polym.* 230 (2020), 115638, <https://doi.org/10.1016/j.carbpol.2019.115638>.
- [35] N. Khanonkon, R. Yoksa, A.A. Ogale, Morphological characteristics of stearic acid-grafted starch compatibilized linear low-density polyethylene/thermoplastic starch blown film, *Eur. Polym. J.* 76 (2016) 266–277, <https://doi.org/10.1016/j.eurpolymj.2016.02.001>.
- [36] J.F. Mendes, R.T. Paschoalin, V.B. Carmona, A.R.S. Neto, A.C.P. Marques, J.M. Marconcini, L.H.C. Mattoso, E.S. Medeiros, L.E. Oliveira, Biodegradable polymer blends based on corn starch and thermoplastic chitosan processed by extrusion, *Carbohydr. Polym.* 137 (2016) 452–458, <https://doi.org/10.1016/j.carbpol.2015.10.093>.
- [37] V.R. Miranda, A.J.F. Carvalho, Blendas Compatíveis de Amido Termoplástico e Polietileno de Baixa Densidade Compatibilizadas com Ácido Cítrico, *Polim 21* (2011) 353–360, <https://doi.org/10.1590/S0104-14282011005000067>.
- [38] S. Shankar, N. Tanomrod, S. Rawdkuen, J.W. Rhim, Preparation of pectin/silver nanoparticles composite films with UV-light barrier and properties, *Int. J. Biol. Macromol.* 92 (2016) 842–849, <https://doi.org/10.1016/j.ijbiomac.2016.07.107>.
- [39] G. Abera, B. Woldeyes, H.D. Demash, G. Miyake, The effect of plasticizers on thermoplastic starch developed from the indigenous Ethiopian tuber crop Anchote (*Coccinia abyssinica*) starch, *Int. J. Biol. Macromol.* 155 (2020) 581–587, <https://doi.org/10.1016/j.ijbiomac.2020.03.218>.
- [40] J. Chen, C. Liu, S. Wu, J. Liang, M. Lei, Enhancing the quality of bio-oil from catalytic pyrolysis of kraft black liquor lignin, *RSC Adv.* 6 (2016), 107970, <https://doi.org/10.1039/c6ra18923g>.
- [41] J.L. Wen, B.L. Xue, F. Xu, R.C. Sun, A. Pinkert, Unmasking the structural features and property of lignin from bamboo, *Ind. Crop. Prod.* 42 (2013) 332–343, <https://doi.org/10.1016/j.indcrop.2012.05.041>.
- [42] M.R.V. Bertolo, L.B.B. Palva, V.M. Nascimento, C.A. Gandin, M.O. Neto, C.E. Drlometer, S.C. Rabelo, Lignins from sugarcane bagasse: renewable source of nanoparticles as Pickering emulsions stabilizers for bioactive compounds encapsulation, *Ind. Crop. Prod.* 140 (2019) 11591, <https://doi.org/10.1016/j.indcrop.2019.11591>.
- [43] C.M. Jaramillo, T.J. Gutiérrez, S. Goyanes, C. Bernal, L. Famá, Biodegradability and plasticizing effect of yerba mate extract on cassava starch edible films, *Carbohydr. Polym.* 151 (2016) 150–159, <https://doi.org/10.1016/j.carbpol.2016.05.025>.
- [44] U. Einhorn-Stoll, H. Kunzek, G. Dongowski, Thermal analysis of chemically and mechanically modified pectins, *Food Hydrocoll.* 21 (2007) 1101–1112, <https://doi.org/10.1016/j.foodhyd.2006.08.004>.
- [45] E. Çakmaklıç Çalgeris, A. Ogan, M.V. Kahraman, N. Kayaman-Apohan, Preparation and drug release properties of lignin–starch biodegradable films, *Starch/Stärke* 64 (2012) 399–407, <https://doi.org/10.1002/star.201100158>.
- [46] W. Yang, J.M. Kenny, D. Puglia, Structure and properties of biodegradable wheat gluten bionanocomposites containing lignin nanoparticles, *Ind. Crop. Prod.* 74 (2015) 348–356, <https://doi.org/10.1016/j.indcrop.2015.05.032>.
- [47] J. Zhou, J. Tong, X. Su, L. Ren, Hydrophobic starch nanocrystals preparations through crosslinking modification using citric acid, *Int. J. Biol. Macromol.* 91 (2016) 1186–1193, <https://doi.org/10.1016/j.ijbiomac.2016.06.082>.
- [48] M.C.G. Pélla, O.A. Silva, M.G. Pellá, A.G. Beneton, J. Caetano, M.R. Simões, D.C. Dragunski, Effect of gelatin and casein additions on starch edible biodegradable films for fruit surface coating, *Food Chem.* 309 (2020), 125764, <https://doi.org/10.1016/j.foodchem.2019.125764>.
- [49] S. Mehboud, T.M. Ali, M. Sheikh, A. Hasnain, Effects of cross linking and/or acetylation on sorghum starch and film characteristics, *Int. J. Biol. Macromol.* 155 (2020) 786–794, <https://doi.org/10.1016/j.ijbiomac.2020.03.144>.
- [50] L.F. Wang, J.W. Rhim, Preparation and application of agar/alginate/collagen ternary blend functional food packaging films, *Int. J. Biol. Macromol.* 80 (2015) 460–468, <https://doi.org/10.1016/j.ijbiomac.2015.07.007>.
- [51] L.F. Ferreira, L.P. Figueiredo, M.A. Martins, L.B. Luvizaro, B.R.B. de blara, C.R. de Oliveira, M.G. Júnior, G.H.D. Tonoli, M.V. Dias, Active coatings of thermoplastic starch and chitosan with alpha-tocopherol/bentonite for special green coffee beans, *Int. J. Biol. Macromol.* 170 (2021) 810–819, <https://doi.org/10.1016/j.ijbiomac.2020.12.199>.
- [52] T. Garrido, A. Etxabide, P. Guerrero, K. de la Caba, Characterization of agar/soy protein biocomposite films: effect of agar on the extruded pellets and compression moulded films, *Carbohydr. Polym.* 151 (2016) 408–416, <https://doi.org/10.1016/j.carbpol.2016.05.089>.
- [53] S. Collazo-Bigliardi, R. Ortega-Toro, A. Chiralt, Improving properties of thermoplastic starch films by incorporating active extracts and cellulose fibres isolated from rice or coffee husk, *Food Packag. Shelf Life* 22 (2019), 100383, <https://doi.org/10.1016/j.fpsl.2019.100383>.
- [54] J. Claude, J. Ubbink, Thermal degradation of carbohydrate polymers in amorphous states: a physical study including colorimetry, *Food Chem.* 96 (2006) 402–410, <https://doi.org/10.1016/j.foodchem.2005.06.003>.
- [55] L.W. Kroch, Caramelisation in food and beverages, *Food Chem.* 51 (1994) 373–379, [https://doi.org/10.1016/0308-8146\(94\)90188-0](https://doi.org/10.1016/0308-8146(94)90188-0).
- [56] G.F. Nogueira, C.T. Soares, R. Cavasini, F.M. Fakhouri, R.A. Oliveira, Bioactive films of arrowroot starch and blackberry pulp: physical, mechanical and barrier properties and stability to pH and sterilization, *Food Chem.* 275 (2019) 417–425, <https://doi.org/10.1016/j.foodchem.2018.09.054>.
- [57] A. Orsuwan, R. Sothernviit, Active banana flour nanocomposite films incorporated with garlic essential oil as multifunctional packaging material for food application, *Food Bioprocess Tech.* 11 (2018) 1199–1210, <https://doi.org/10.1007/s11947-018-2089-2>.
- [58] L.F. Wang, J.W. Rhim, Grapefruit seed extract incorporated antimicrobial LDPE and PLA films: effect of type of polymer matrix, *LWT - Food Sci. Technol.* 74 (2016) 338–345, <https://doi.org/10.1016/j.lwt.2016.07.066>.